Crystal Structure and Enzyme Mechanism of Δ^5-3-Ketosteroid Isomerase from *Pseudomonas testosteroni*[†,‡]

Hyun-Soo Cho,[§] Gildon Choi,[||] Kwan Yong Choi,[§,||] and Byung-Ha Oh*[,§]

Department of Life Science, School of Environmental Engineering, and Center for Biofunctional Molecules, Pohang University of Science and Technology, Pohang, Kyungbuk, 790-784, South Korea

Received January 21, 1998

ABSTRACT: Bacterial Δ^5-3-ketosteroid isomerase (KSI) from *Pseudomonas testosteroni* has been intensively studied as a prototype for understanding an enzyme-catalyzed allylic rearrangement involving intramolecular proton transfer. Asp^{38} serves as a general base to abstract the proton from the steroid C4-H, which is a much stronger base than the carboxyl group of this residue. This unfavorable proton transfer requires 11 kcal/mol of energy which has to be provided by favorable interactions between catalytic residues and substrate in the course of the catalytic reaction. How this energy is provided at the active site of KSI has been a controversial issue, and inevitably the enzyme mechanism is not settled. To resolve these issues, we have determined the crystal structure of this enzyme at 2.3 Å resolution. The crystal structure revealed that the active site environment of *P. testosteroni* KSI is nearly identical to that of *Pseudomonas putida* KSI, whose structure in complex with a reaction intermediate analogue we have determined recently. Comparison of the two structures clearly indicates that the two KSIs should share the same enzyme mechanism involving the stabilization of the dienolate intermediate by the two direct hydrogen bonds to the dienolate oxyanion, one from Tyr^{14} OH and the other from Asp^{99} COOH. Mutational analysis of the two residues and other biochemical data strongly suggest that the hydrogen bond of Tyr^{14} provides the more significant contribution than that of Asp^{99} to the requisite 11 kcal/mol of energy for the catalytic power of KSI.

KSI from *Pseudomonas testosteroni* catalyzes the allylic isomerization of a variety of Δ^5-3-ketosteroids to Δ^4-3-ketosteroids by a stereospecific intramolecular transfer of the 4β-proton to the 6β position [**1**] (*1*). The reaction consists of enolate formation and reketonization that are employed by a wide variety of biologically important reactions of carbonyl compounds. The enzyme, a homodimer in solution, is one of the most proficient enzymes enhancing the catalytic rate by a factor of 11 orders of magnitude (*2*). Site-directed mutagenesis and kinetic studies (*3*−*5*) identified two residues critical for the catalysis. Asp^{38} was identified as the general base abstracting the 4β-proton of the steroid substrate and Tyr^{14} as the general acid protonating or providing a hydrogen bond (H-bond) to the dienolate intermediate:

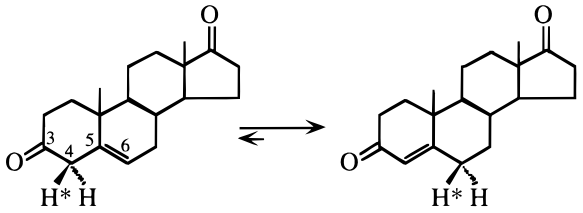

[1]

The proton transfer from the steroid C4-H (pK_a = 12.7) (*6*) to Asp^{38} (pK_a = 4.7) is energetically unfavorable and requires about 11 kcal/mol for transition-state stabilization which coincides with the experimentally obtained value (*7*). Such unfavorable general acid/base proton transfers are found in many enzymes, and how the active sites of enzymes are able to provide a requisite amount of energies is a major mechanistic question. A conventional account for these energies is formation of multiple favorable interactions of moderate strength at the active site (*8*). For KSI, three to four H-bonds would be necessary to account for the required energy. However, Tyr^{14} had been the only residue known to provide a H-bond to the reaction intermediate. Recently, a mutational analysis directed by the solution structure of *P. testosteroni* KSI (TI) suggested that Asp^{99} is a critical residue serving as a general acid with an unusually high pK_a

[†] This study made use of the X-ray Facility at Pohang Light Source and was supported by the R & D Promotion Center for Agriculture, Forestry and Fishery in Korea and in part by the Basic Science Research Fund of POSTECH and by the Research Center for New Bio-Materials in Agriculture.

[‡] The coordinates have been deposited with the Brookhaven Protein Data Bank (code 8CHO).

* To whom correspondence should be addressed (Tel 82-562-279-2289; Fax 82-562-279-2199; e-mail bhoh@vision.postech.ac.kr).

[§] Department of Life Science and School of Environmental Engineering.

[||] Center for Biofunctional Molecules.

S0006-2960(98)00161-5 CCC: $15.00
Published on Web 05/20/1998

of 9.5 (*9*). Independently, the crystal structure of a homologous *Pseudomonas putida* KSI (PI) in complex with an intermediate-analogue equilenin revealed that Asp^{99} COOH as well as Tyr^{14} OH (TI numbering is used for all the residues throughout the text) is involved in a direct H-bond with the oxyanion of the analogue (*10*). The D99L mutation in PI resulted in a substantial decrease in k_{cat}, confirming that Asp^{99} is a newly identified catalytic residue. While TI has been studied extensively for more than three decades, PI has been much less studied since its gene cloning in 1994 (*11*). PI is composed of 131 residues, 6 amino acids more than TI. The two enzymes share 44 identically conserved amino acids including the three catalytic residues (Tyr^{14}, Asp^{38}, Asp^{99}).

The low-resolution solution structure of TI ambiguously supported mechanism I in which Tyr^{14} OH and Asp^{99} COOH are directly involved in the stabilization of the dienolate intermediate and led to a conclusion that the 11 kcal/mol of energy is provided by the two medium-strength hydrogen bonds (4−5 kcal/mol) from Tyr^{14} and Asp^{99} along with an unexplained catalytic role of Phe^{101} (2 kcal/mol) following the observation of 270-fold reduction in k_{cat} by the F101A substitution (*12*). The 1.9 Å crystal structure of PI did not support the catalytic role of Phe^{101} in TI since the corresponding residue, Met^{101} in PI, revealed no interaction with the bound inhibitor (*10*). However, due to the differences in the amino acid sequences of the two KSIs, the possibility of two different ways of stabilizing the reaction intermediate could not be ruled out.

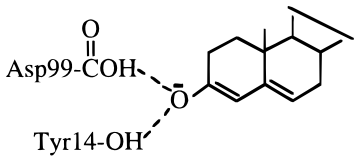

mechanism I

In the presence of dihydroequilenin or estradiol 17β-hemisuccinate, an NMR study detected a highly deshielded proton resonance at 18.15 ppm (*13*). Such resonances have been typically observed for a number of H-bonds between two heteroatoms with an equal pK_a in the apolar environment (*14*) and attributed to the formation of unusually strong low-barrier hydrogen bonds (LBHBs) (*14*−*17*). The 18.15 ppm was originally assigned to the Tyr^{14} OH proton engaged in a strong LBHB with the oxyanion of the inhibitors. The H-bond strength was estimated at >7.1 kcal/mol on the basis of a comparison of the rates of dissociation of the reaction intermediate from Y14F and D38N mutants of TI (*13*). Later, mainly on the basis of the disappearance of the resonance upon substitution of either Y14F or D99A, it was reassigned to the Asp^{99} COOH proton which was assumed to be involved in a LBHB with Tyr^{14} OH (*18*). The study led to a catalytic dyad mechanism in which LBHB from Asp^{99} strengthens general acid catalysis by Tyr^{14} as in mechanism II.

The crystal structures of PI and its complex with equilenin provided detailed pictures of the active site residues and their interactions with the inhibitor and, along with the NMR study (*13*), led to a conclusion that a strong LBHB (~7 kcal/mol) from Tyr^{14} and a medium-strength H-bond (~4 kcal/mol) from Asp^{99} are the sources of 11 kcal/mol of the transition-state stabilization. The conclusion is not consistent with

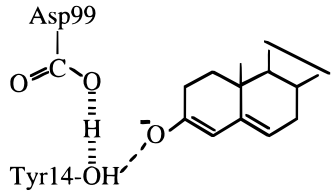

mechanism II

those derived from the two independent NMR studies, both of which are not consistent either. A lack of an accurate high-resolution structure of TI is primarily responsible for the confusion. We fortunately crystallized TI, which has been resistant to yield suitable crystals for many years, and determined the structure of the enzyme at 2.3 Å resolution. This, in conjunction with the structure of PI in complex with equilenin, settles the confusion and conflict in the catalytic mechanism and the catalytic energy sources of this heavily studied enzyme.

EXPERIMENTAL PROCEDURES

Protein Purification. The procedures for overexpression and purification of TI were carried out as described previously (*19*) with a slight modification. The TI gene was subcloned into *Eco*RI and *Hin*dIII sites of pKK223-3 to construct a recombinant plasmid, pKSI-TI. TI was overexpressed in the *Escherichia coli* strain BL21 (DE3) transformed with pKSI-TI when induced with 0.5 mM isopropyl β-D-thiogalactopyranoside. The crude lysate containing overexpressed TI was directly applied onto a deoxycholate affinity column equilibrated with 40 mM potassium phosphate buffer (pH 7.0) containing 1 mM EDTA. After the column was washed, the bound proteins containing TI were eluted with 50 mM Tris-HCl buffer (pH 7.0) containing 25% ethanol and finally separated by Superose 12 column chromatography (Pharmacia). The purified TI showed a homogeneous single band on SDS−PAGE and was concentrated by Centricon-10 (Amicon) for crystallization.

Crystallization. KSI crystals were grown at 12 °C from 1.3 M ammonium sulfate, 3−5% poly(ethylene glycol) 400 (PEG400), and 0.1 M HEPES (pH 7.5) in hanging drops. Two microliters of the final protein sample (5 mg/mL) was mixed with an equal volume of the precipitant solution. The crystals tend to grow in clusters of many tiny crystals. Only occasionally, large single crystals (0.2 × 0.2 × 0.5 mm) in the form of a hexagonal rod were obtained. The crystals belong to the space group $P6_522$ with unit cell dimensions of $a = b = 61.68$ Å and $c = 143.60$ Å. In this crystal form, the molecular 2-fold axis coincides with a crystallographic 2-fold axis, and one subunit of the enzyme is contained in the asymmetric unit.

Data Collection, Structure Determination, and Refinement. Diffraction data (95% complete up to 2.3 Å) were measured on a DIP2020 area detector with graphite monochromated Cu Kα X-rays generated by a MacScience M18XHF rotating anode generator operated at 90 mA and 50 kV at room temperature. Data reduction, merging, and scaling were accomplished with the programs DENZO and SCALEPACK (*20*). The systematic absences along the *c* axis indicated the presence of either a 6_1 or 6_5 screw axis. The structure was solved by the molecular replacement protocol in the X-PLOR program package (*21*) using the coordinates of PI.

At the beginning, rotation searches using one protomer of PI as a model did not yield a correct solution. The reflection data were reprocessed in a lower space group *P*6, and a rotation search using the dimeric model of PI yielded an unambiguous rotation solution. Two translation searches were carried out along the *xy*-plane for the space groups $P6_1$ and $P6_5$, respectively. The space group $P6_5$ yielded a strong translation function peak resolving the ambiguity of the space group. Taking a monomer from the dimeric translation solution, a translation search along the *z*-axis was carried out with the data processed as the space group $P6_522$ to determine the position along the *z*-axis. The search found a correct solution as it was confirmed by favorable crystal packing interactions between symmetry mates. The rigid body refinement (20 steps of conjugate gradient minimization against reflections at 10−3.0 Å resolution) of the translation solution resulted in an *R*-factor of 48.3%. Five percent of the reflections was set aside for monitoring R_{free}. An atomic positional refinement lowered the $R_{working}$ to 39.8% at 10.0−2.5 Å resolution. At this point, guided by the $2F_o - F_c$ and $F_o - F_c$ electron density maps, many amino acids of PI were replaced according to the amino acid sequence of TI. Loop regions and N-terminal and C-terminal regions containing deletions compared with the PI sequence required refitting of both side chains and backbones. Particularly, residues 75−81 containing a deletion of glycine in TI required substantial refitting. After multiple rounds of manual fitting and positional refinement, the current model containing a total of 29 water molecules exhibits an $R_{working}$ of 20.5% (R_{free} = 27.1%) for reflections (1σ above) at 10.0−2.3 Å resolution. All the residues in the final structure are within the allowed regions in the Ramachandran plots. Root-mean-square deviations of bond lengths and angles are 0.012 Å and 1.615°, respectively.

RESULTS AND DISCUSSION

Crystallization. Although X-ray crystallographic study of TI dates back to 1971, obtaining suitable crystals of TI has been elusive. The early study on the hexagonal crystal form suffered from an unsuitable unit cell dimension of 504 Å and led to an erroneous TI structure at 6 Å (*22*). In retrospect, we overcame this problem by including 3−5% PEG400 in the crystallization condition where ammonium sulfate was the major precipitant as in the early study. During the refinement, two long continuous electron densities, adjacent to each other, were found at an interface of two TI molecules (data not shown). We interpreted it as the electron density of poly(ethylene glycol) with seven $-CH_2O-$ units. This corresponds to a molecular mass of 342 Da, slightly below the average molecular mass of PEG400. It mediates weak interactions between the active site cavity of one molecule and Met[1], His[6], and Ala[106] of an adjacent molecule. The incorporation of PEG400 appears to be a key resulting in a crystal packing favorable for the structure determination which was not obtained in the early studies (*23*, *24*).

Overall Structure. The structure of TI is a conical closed barrel formed by a highly curved β-sheet and three α-helices (Figure 1). An widely open end of the structure is the entrance to the active site cavity tapering off to a blocked wall inaccessible from the other narrow end. The residues that form the secondary structures are Thr[3]−Ala[20] (α-helix A1), Leu[23]−Leu[29] (α-helix A2), Ala[34]−Pro[39] (β-strand B1), Pro[44]−Ser[46] (β-strand B2), Thr[48]−Leu[59] (α-helix A3), Leu[63]−Val[74] (β-strand B3), Glu[77]−Tyr[88] (β-strand B4), Arg[91]−Phe[103] (β-strand B5), and Val[110]−Ala[123] (β-strands B6 and B7). A bulge, composed of Phe[116]-Gly[117]-Glu[118]-Lys[119]-Asn[120], is found between strands B6 and B7. The three central antiparallel β-strands (strands B3, B4, and B5) are highly curved and span the entire monomeric structure. The curvature of strand B3 is due to a bend at the sequence of Thr[68]-Gln[69]-Glu[70] which forms a β-bulge. A relatively sharp kink at Ala[81] is observed, which is responsible for the curvature of strand B4. The longest β-strand B5 shows a smooth bend at residues Pro[97]-Ile[98].

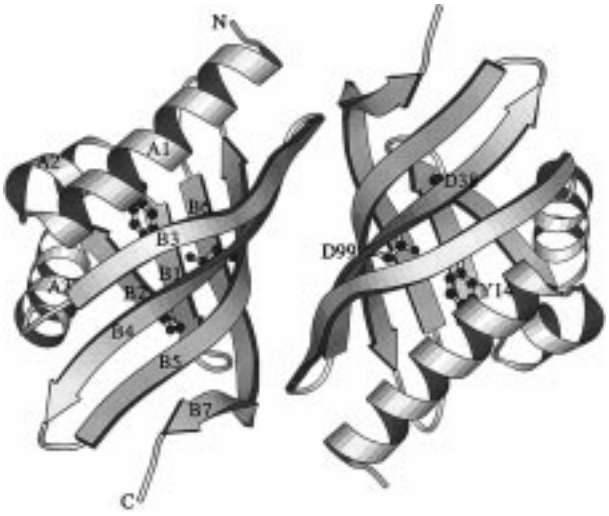

FIGURE 1: Dimeric structure of KSI viewed roughly along the molecular 2-fold axis. The three major catalytic residues are shown in ball-and-stick model. Strand B7 is a continuation of strand B6 considering a β-bulge between the two.

A narrow and long patch of the β-sheet of each protomer forms a dimer interface. The dimer interactions are mostly between side chains and are mostly hydrophobic. A total of 20 residues of one protomer are within 3.8 Å from the other protomer. These residues are Val[40], Thr[68], Gln[69], Glu[70], Val[71], Arg[72], Ala[73], Val[74], Glu[77], Ala[81], Ala[96], Pro[97], Ile[98], Arg[113], Leu[115], Phe[116], Gly[117], Lys[119], Asn[120], and His[122]. It was interesting to note that both of the two β-bulges (residues 68−70 and 116−120) participate in the dimer interactions. Apparently, the β-bulge structures are stabilized, at least partly, by the dimer interactions. A few electrostatic interactions between side chains are found for Thr[68], Glu[70], and Glu[77] of one protomer interacting with Gln[69], (Asn[120], His[122]), and Arg[113], respectively, of the other protomer. In addition, four bound water molecules at the dimer interface mediate intersubunit H-bonds between Thr[68], Arg[72], His[100], and Arg[113]. In contrast to the absence of main chain H-bonds between the protomers in the solution structure of *P. testosteroni* KSI (*9*), the carbonyl oxygens of Val[71] and Ala[96] of one protomer are involved in direct H-bonds with the side chains of Asn[120] and Arg[72] of the other protomer, respectively.

Active Site Environment. In the active site of TI, Tyr[14], Tyr[55], a bound water molecule (W[504]), and Asp[99] form a H-bonded network, while Asp[38], located at the opening of the active site cavity, is beyond a H-bond distance from these residues (Figure 2). The most prominent feature of the active

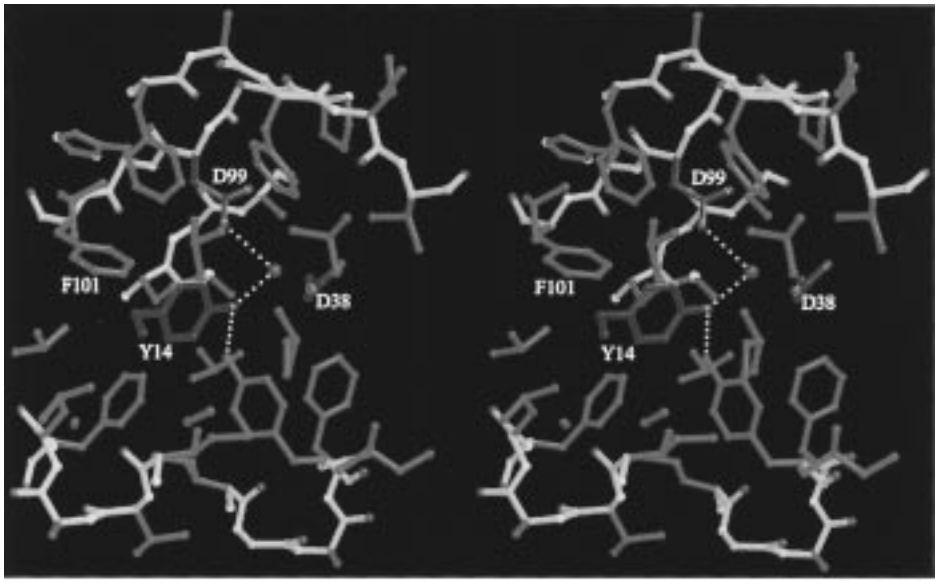

FIGURE 2: Stereo diagram showing the three catalytic residues in green. The protein backbones are indicated in coral. For clarity only side chains are shown for many residues. The residues lining the active site and surrounding the catalytic residues are in magenta. They are all apolar residues except for Tyr^{55} ,which is engaged in a H-bond with Tyr^{14}. The H-bonds are indicated by dotted lines. Phe^{101}, which has been suggested to play an "unexplained" catalytic role, is labeled.

site environment of TI, in common with PI, is that the active site residues except Asp^{38} are surrounded and blocked from bulk solvent by apolar amino acids, specifically Val^{11}, Val^{15}, Ala^{17}, Leu^{18}, Ile^{26}, Val^{27}, Leu^{29}, Phe^{30}, Ala^{34}, Val^{36}, Ile^{51}, Phe^{54}, Leu^{59}, Val^{65}, Phe^{80}, Phe^{82}, Pro^{97}, Phe^{101}, Val^{109}, Met^{112}, and Ala^{114}. These apolar residues are all identically or homologously substituted in PI. The overall structure and the disposition of active site residues of the two KSIs are very similar, as indicated by the superposition of the two structures with a small root-mean-square difference (rms) of 0.667 Å (Figure 3). The structure of PI in complex with equilenin revealed that the active site residues except Asp^{38} are surrounded by the apolar residues and the hydrophobic inhibitor with the solvent accessibility of zero. No water molecule is found at the active site, and thus the access of bulk solvent during the enzyme catalysis should be blocked by the layer of the apolar residues and the steroid substrate. These structural observations elucidate that the steroid conversion by the two enzymes is carried out in a highly apolar environment.

Previously, pH-dependent enzymatic activity assay (*25*) and fluorescence titration of Tyr^{14} (*26*) suggested an unidentified active site residue with a pK_a of 9.5 and in a close distance to Tyr^{14}. The titratable active site residue Asp^{99} is surrounded by apolar side chains of Phe^{80}, Phe^{82}, Pro^{97}, Phe^{101}, Met^{112}, and Ala^{114} (Figure 2). Such apolar environment should elevate the pK_a of Asp^{99}. Moreover, the closest distance between Asp^{99} and Tyr^{14} is 3.87 Å, indicating that Asp^{99} should be responsible for the previous observations. The structure of PI in complex with equilenin revealed that the oxyanion of the inhibitor interacts directly with Asp^{99} as well as Tyr^{14} by displacing W^{504}, which is involved in H-bonds with the two residues in the uninhibited state of the enzyme (Figures 2 and 3). The high pK_a of Asp^{99} is to ensure the favorable interaction between its protonated side chain and the oxyanion of the dienolate intermediate. Among the active site residues, Tyr^{55} contributes minimally to the catalysis since Y55F mutation in TI causes only a 4-fold decrease in k_{cat} (*27*). Consistently, Tyr^{55} does not interact with the bound inhibitor in the structure of the PI−equilenin complex.

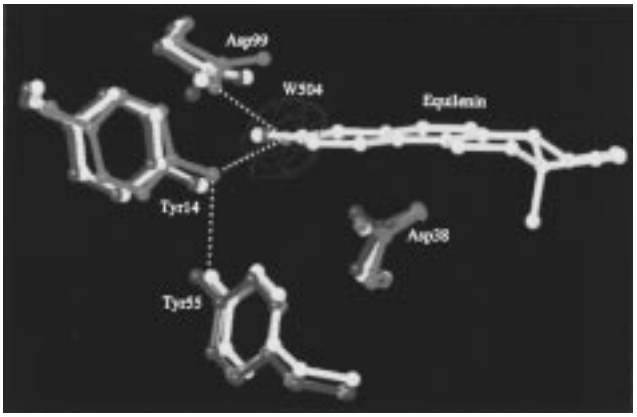

FIGURE 3: Superposition of structures of TI (magenta), PI (green), and the PI−equilenin complex (yellow). The Cα atoms of residues 6−59, 63−74, 80−87, and 91−124 were used for the superpositions. Four regions (the N- and C-termini and two loop regions) were omitted because of irrelevant conformational differences resulting from the six amino acid deletions in TI, and one loop region (residues 88−90) was omitted because of a conformational difference due to crystal packing. The rms difference after the superposition of TI and PI is 0.667 Å, and that of the TI and PI−equilenin complex is 0.675 Å. Water molecule W^{504}, located at nearly the same position in both TI and PI, is shown along with the $2F_o - F_c$ electron density map calculated with the final model of TI using data between 10 and 2.3 Å resolution and contoured at 1.3σ. Program O was used for the figure (*29*).

Seemingly Catalytic Residue Phe[101]. Phe^{101} is not a conserved residue, and the corresponding residue Met^{101} in PI does not interact with the bound inhibitor in the structure of the PI−equilenin complex. A superposition of the structures of TI and the PI−equilenin complex shows that Phe^{101} does not interact with equilenin either (Figure 3), suggesting that Phe^{101} in TI is not a catalytic residue. A simple modeling experiment was carried out on the 2.3 Å TI structure to explain the previously observed 270-fold

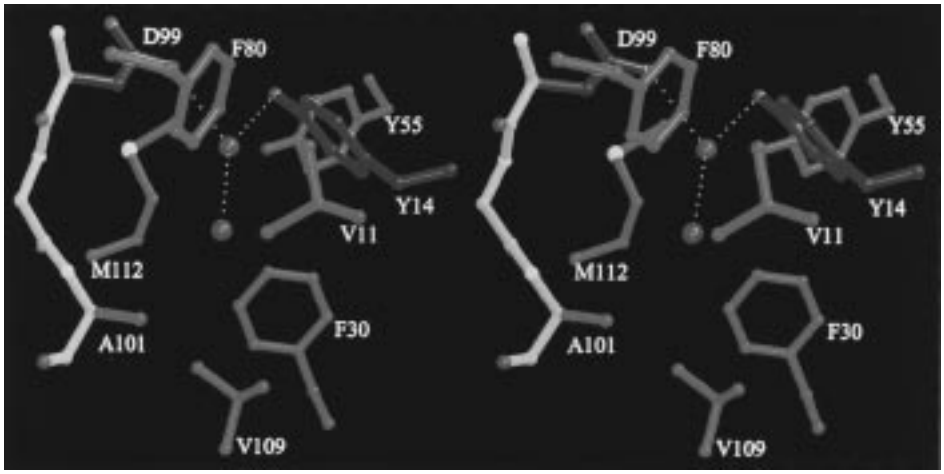

FIGURE 4: Stereo diagram of two water molecules modeled in the empty space generated by F101A mutation. Nearby residues are shown in magenta except Tyr^{14} and Asp^{99}, which are shown in green. Expected H-bonds are indicated by dotted lines. The program Molscript (*30*) was used for generating Figures 1, 2, and 4.

reduction in k_{cat} by the F101A mutation. Phe^{101} is one of the residues surrounding Asp^{99} contributing to the elevation of the pK_a of Asp^{99} (Figure 2). The F101A mutation leaves an empty space into which two water molecules can be modeled without a steric clash (Figure 4). One of the two water molecules is involved in hydrogen bonds with the side chains of Tyr^{14} and Asp^{99} and with the other water molecule. The incorporation of water molecules at this position would increase the polarity of the active site cavity, resulting in lowering the pK_a of Asp^{99} and in weakening the strength of the H-bonds between the catalytic residues and the reaction intermediate. Another possible explanation for the effect of F101A mutation is that the side chain of Phe^{101} plays a role in propping the side chain of Asp^{99} in a proper conformation ready to interact with the incoming steroid substrates, which would not be supported by the alanine substitution.

Correct Enzyme Mechanism of KSI. The disappearance of the 18.15 ppm resonance upon D99A mutation was the main basis for the proposal of the catalytic dyad shown in mechanism II and for the reassignment of the resonance to Asp^{99} COOH. Without recourse to the catalytic dyad, the disappearance of the resonance can be explained by a modeling study on the structure of TI. A water molecule can be modeled into the space generated by the mutation (data not shown). Increased solvent accessibility near the H-bond between Tyr^{14} OH and the dienolate intermediate would decrease the H-bond strength as the F101A mutation does. It should also be noted that unusually downfield-shifted resonances were observed only in the absence of a water molecule (*14*). A superposition of the structures of TI and PI reveals that the spatial arrangement of the three catalytic residues (Tyr^{14}, Asp^{38}, Asp^{99}) is nearly identical in the two enzymes. Even the existence of W^{504}, a bound water molecule between Tyr^{14} and Asp^{99} (Figure 3), is the same. A superposition of TI and the PI−equilenin complex shows that the inhibitor should bind to TI by replacing W^{504} and interacting with both Tyr^{14} and Asp^{99}, as it does to PI (Figure 3). These structural data indicate that both KSIs share the same catalytic mechanism where the developing negative charge on the C3 oxygen of the reaction intermediate is stabilized as shown in mechanism I.

Energetic Contribution. The required 11 kcal/mol of energy for the abstraction of the steroid C3 proton appears to be met by the two direct H-bonds provided by Tyr^{14} and Asp^{99}. It is highly likely that Tyr^{14} provides a stronger H-bond than Asp^{99} because a mutant TI containing an Y14F mutation caused a 50 000-fold decrease (*27*), while the D99A substitution resulted in a 5000-fold decrease in k_{cat} (*9*). The net mutational effect of the D99A on k_{cat} should be less than the measured value since the D99A mutation is expected to weaken the H-bond of Tyr^{14} due to the access of water molecules near Tyr^{14} OH. The stronger H-bond of Tyr^{14} is likely due to a pK_a similar to that of the dienolate intermediate. By UV and fluorescence titration, the pK_as of Tyr^{14} and Asp^{99} were measured in the absence of a steroid substrate as 11 and 9.5, respectively (*26*). The spectroscopically measured pK_a of the C3 oxygen of the steroid dienolate intermediate in water is 10.0 (*28*). In the highly apolar active site of TI, the pK_a of the dienolate intermediate could be elevated and become similar to that of Tyr^{14} OH. It was experimentally shown that the difference in the H-bond strengths correlates with the difference in pK_as of two groups involved in a H-bond, being the maximum at $\Delta pK_a = 0$ (*8*). Under the condition of $\Delta pK_a = 0$, a H-bond as strong as 6.3 kcal/mol was detected between 4-nitrophenol and 4-nitrophenolate in tetrahydrofuran (*8*). Since H-bond strength is inversely proportional to the dielectric constant of a medium, formation of an unusually strong H-bond is expected in a low dielectric milieu such as the active site of KSI. In small molecular systems, highly downfield-shifted resonances of H-bonds were detected in the absence of polar solvent and under a condition of matched pK_as of the two groups involved in charged H-bonds. The H-bond between Tyr^{14} OH and the dienolate intermediate should mimic the small molecular system, and thus the 18.15 ppm ^{1}H resonance of TI detected in the presence of intermediate analogues (*13*) is likely to be from Tyr^{14} OH. Confusingly, the original assignment of the resonance to Tyr^{14} OH was negated, and it was reassigned to Asp^{99} COOH, leading to the conclusion that Asp^{99} does not interact directly with the reaction intermediate as in mechanism II. However, the reassignment was based on an indirect elimination comparing NMR spectra of the wild-type and mutant TIs. The existence of nuclear Overhauser effects (NOE) between Asp^{99} Hβs and Tyr^{14} Hϵ was presented as evidence for the proximity of the side chain of Asp^{99} to the aromatic ring of Tyr^{14}, which was assumed

to be unobservable in the H-bonding scheme in mechanism I. However, the crystal structure of TI, which supports mechanism I, shows that those protons are indeed in close proximity to each other. The interproton distances between the two Asp^{99} β protons and Tyr^{14} Hϵ are 4.76 and 5.0 Å, when measured on TI coordinates which were refined including all hydrogens explicitly using the program X-PLOR (*21*). Within the coordinates error, these distances well explain the observation of the weak NOE cross-peaks between the two residues. More importantly, the distance between Tyr^{14} Oη and Asp^{99} Oδ2 is 3.87 Å, which is too far for H-bond formation. It is unlikely that the distance is shortened upon substrate or inhibitor binding, because Tyr^{14} and Asp^{99} were shown to remain at nearly the same position upon the binding of equilenin (Figure 3) (*10*). A simple modeling experiment, where the side chain torsion angles of Tyr^{14} and Asp^{99} were manipulated, also showed that the two residues cannot be brought within a H-bond distance without causing steric clashes with nearby residues and breaking the H-bond between Tyr^{14} and Tyr^{55}. The assignment of the 18.15 ppm resonance needs to be reevaluated, relying on a reinterpretation of the NOE peaks and/or a direct resonance assignment protocol.

In conclusion, the accurate 2.3 Å structure of TI indicates that Phe^{101} is not a catalytic residue and that Tyr^{14} and Asp^{99} COOH should be directly involved in the stabilization of the dienolate intermediate. Both KSIs employ a strategy of H-bond strengthening by embedding charged H-bonds between catalytic residues and its target in the highly apolar milieu of the active site. The structure elucidation provides a framework on which physicochemical experiments can be designed for correct estimation of the H-bond strengths of Tyr^{14} and Asp^{99}.

REFERENCES

1. Batzold, F. H., Benson, A. M., Covey, D. F., Robinson, C. H., and Talalay, P. (1976) *Adv. Enzyme Regul. 14*, 243−267.
2. Radzicka, A., and Wolfenden, R. (1995) *Science 267*, 90−93.
3. Xue, L., Kuliopulos, A., Mildvan, A. S., and Talalay, P. (1991) *Biochemistry 30*, 4991−4997.
4. Xue, L., Talalay, P., and Mildvan, A. S. (1991) *Biochemistry 30*, 10858−10865.
5. Holman, C. M., and Benisek, W. F. (1994) *Biochemistry 33*, 2672−2681.
6. Hawkinson, D. C., Pollack, R. M., and Ambulos, N. P., Jr. (1994) *Biochemistry 33*, 12172−12183.
7. Hawkinson, D. C., Eames, T. C., and Pollack, R. M. (1991) *Biochemistry 30*, 10849−10858.
8. Shan, S., Loh, S., and Herschlag, D. (1996) *Science 272*, 97−101.
9. Wu, Z. R., Ebrahimian, S., Zawrotny, M. E., Thornburg, L. D., Perez-Alvarado, G. C., Brothers, P., Pollack, R. M., and Summers, M. F. (1997) *Science 276*, 415−418.
10. Kim, S. W., Cha, S.-S., Cho, H.-S., Kim, J.-S., Ha, N.-C., Cho, M.-J., J., S., Kim, K.-K., Choi, K. Y., and Oh, B.-H. (1997) *Biochemistry 36*, 14030−14036.
11. Kim, S. W., Kim, C. Y., Benisek, W. F., and Choi, K. Y. (1994) *J. Bacteriol. 176*, 6672−6676.
12. Brothers, P. N., Blotny, G., Qi, L., and Pollack, R. M. (1995) *Biochemistry 34*, 15453−15458.
13. Zhao, Q., Abeygunawardana, C., Talalay, P., and Mildvan, A. S. (1996) *Proc. Natl. Acad. Sci. U.S.A. 93*, 8220−8224.
14. Gerlt, J. A., and Gassman, P. G. (1993) *J. Am. Chem. Soc. 115*, 11552−11568.
15. Gerlt, J. A., and Gassman, P. G. (1993) *Biochemistry 32*, 11943−11952.
16. Cleland, W. W., and Kreevoy, M. M. (1994) *Science 264*, 1887−1890.
17. Frey, P. A., Whitt, S. A., and Tobin, J. B. (1994) *Science 264*, 1927−1930.
18. Zhao, Q., Abeygunawardana, C., Gittis, A. G., and Mildvan, A. S. (1997) *Biochemistry 36*, 14616−14626.
19. Kim, S. W., and Choi, K. Y. (1995) *J. Bacteriol. 177*, 2602−2605.
20. Otwinowski, Z. (1993) in *Proceedings of the CCP4 Study Weekend* (Sawyer, L., et al., Eds.) pp 56−62, SERC Daresbury Laboratory, Warrington, U.K.
21. Brünger, A. T. (1992) *X-PLOR Version 3.0*, Yale University, New Haven, CT.
22. Westbrook, E. M., Piro, O. E., and Sigler, P. B. (1984) *J. Biol. Chem. 259*, 9096−9103.
23. Westbrook, E. M. (1976) *J. Mol. Biol. 103*, 659−664.
24. Westbrook, E. M., Sigler, P. B., Berman, H., Glusker, J. P., Bunick, G., Benson, A., and Talalay, P. (1976) *J. Mol. Biol. 103*, 665−667.
25. Weintraub, H., Alfsen, A., and Baulieu, E.-E. (1970) *Eur. J. Biochem. 12*, 217−221.
26. Li, Y. K., Kuliopulos, A., Mildvan, A. S., and Talalay, P. (1993) *Biochemistry 32*, 1816−1824.
27. Kuliopulos, A., Mildvan, A. S., Shortle, D., and Talalay, P. (1989) *Biochemistry 28*, 149−159.
28. Zeng, B., and Pollack, R. M. (1991) *J. Am. Chem. Soc. 113*, 3838−3842.
29. Jones, T. A., and Kjeldgaard, M. (1993) *O version 5.9. The Manual*, Uppsala University, Uppsala, Sweden.
30. Kraulis, P. J. (1991) *J. Appl. Crystallogr. 24*, 946−950.

BI9801614